(ISSN: 0973-7049(P))

The Bioscan
AN INTERNATIONAL QUARTERLY JOURNAL OF LIFE SCIENCES

21(4): S.I (4),863-875, 2026

www.thebioscan.com

Cyanobacterial Diversity associated to the Rock-Cut Caves of Nashik, Maharashtra, India

Zirwal M. R.[1,2], Meshram B. G.[2*]

[1]Department of Botany, Yashwantrao Chavan College of Science, Vidyanagar, Karad 415124
[2]Department of Botany, Savitribai Phule Pune University, Ganeshkhind, Pune 411007
*Corresponding Author: balu.meshram@gmail.com

DOI: https://doi.org/10.63001/tbs.2026.v21.i04.S.I(4).pp863-875

KEYWORDS
Cyanobacteria; lithophytic cyanobacteria; rock-cut caves; cultural heritage; biofilm; biodeterioration; morphological taxonomy

Received on: 12 Aug 2026

Accepted on: 28 Oct 2026

Published on: 5 Nov 2026

Abstract

Cyanobacterial biofilms are pioneering communities on lithic surfaces and may contribute to discoloration, moisture, mineral interactions and biodeterioration of cultural heritage. The present study documents the morphological diversity of cyanobacteria associated with five rock-cut cave complexes of Nashik District, Maharashtra, India: Chamar Leni, Pandav Leni, Jain Caves, Trigalwadi Caves and Ankai Caves. Samples were collected from moist and wet rock walls, floors, sculptures, soil-associated surfaces, water-contact zones and nearby subaerophytic substrates. Environmental observations included temperature, pH and relative humidity. The compiled checklist comprised 55 morphotaxa representing 18 genera and 72 site occurrences. Coccoid forms represented 25 taxa (45.5%), non-heterocystous filamentous forms traditionally grouped as Oscillatoriales represented 13 taxa (23.6%) and heterocystous forms represented 17 taxa (30.9%). Pandav Leni exhibited the highest observed richness (33 taxa), followed by Ankai (18), Jain (8), Chamar Leni (7) and Trigalwadi (6). Nostoc commune was recorded at all five study sites, whereas Aphanothece castagnei and Gloeocapsa compacta each occurred at three sites. The assemblage contained numerous taxa with mucilaginous sheaths, thick envelopes, false branching or heterocysts, traits consistent with persistence under fluctuating moisture and high irradiance. The results support previous Indian and International observations that cyanobacteria can form persistent lithophytic biofilms on heritage stone surfaces. However, because identification in the present study was morphology-based, the reported species should be regarded as morphotaxa pending molecular confirmation. Future work should integrate 16S rRNA/16S–23S ITS sequencing, quantitative abundance measurements, stone physicochemistry and seasonal monitoring to resolve cryptic diversity and strengthen conservation applications.

1. INTRODUCTION

Rock-cut caves and stone monuments provide special microhabitats for phototrophic microorganisms. Their surfaces can experience strong spatial variation in illumination, temperature, moisture, pH, surface roughness and nutrient availability. Cyanobacteria are particularly successful on lithic substrates because many taxa tolerate desiccation, high irradiance, nutrient limitation and repeated wetting and drying. Once established, cyanobacterial cells and filaments may produce extracellular polymeric substances (EPS), pigments and mineral-binding compounds that promote attachment and persistence on stone surfaces (Pointing & Belnap, 2012; Gaylarde, 2020).

The significance of cyanobacteria on cultural heritage is not restricted to their presence as a taxonomic component. Phototrophic biofilms can alter the appearance of stone through green, blue-green, brown, black or reddish pigmentation and can modify the stone–atmosphere interface. EPS may retain water and inorganic particles, while microbial growth in pores and microfractures can contribute to physical and chemical alteration. Reviews of stone biodeterioration have therefore emphasized the importance of identifying the organisms colonizing heritage substrates before conservation interventions are designed (Scheerer *et al.*, 2009; Negi & Sarethy, 2019).

Indian heritage structures provide numerous examples of lithophytic cyanobacterial communities. Keshari and Adhikary (2013) characterized cyanobacteria from stone monuments at Santiniketan, and Keshari and Adhikary (2014) reported 24 cyanobacterial species belonging to 11 genera from Indian monuments, building facades and caves. Their molecular analyses also demonstrated that morphology-based identification of cyanobacteria from stressed lithic environments can be difficult and that tropical populations may show distinct phylogenetic patterns. Other studies have demonstrated the importance of EPS in monument-associated cyanobacteria and the capacity of stress-tolerant taxa such as Scytonema to persist under intense environmental stress (Rossi *et al.*, 2012; Keshari *et al.*, 2021).

Nashik District contains an important concentration of ancient rock-cut caves, including the Pandav Leni/Trirashmi complex and several cave groups in the surrounding hill systems. The Government of Maharashtra describes Pandav Leni as a major group of ancient rock-cut caves on Trirashmi Hill, with 24 caves and substantial carved stone surfaces that have persisted for centuries. Such surfaces provide suitable locations for studying the interaction between phototrophic microbial colonization and cultural stone substrates.

Despite the ecological and conservation relevance of cyanobacteria on Indian monuments, site-specific information for the cave complexes of Nashik remains limited. The present

(ISSN: 0973-7049(P))

The Bioscan
AN INTERNATIONAL QUARTERLY JOURNAL OF LIFE SCIENCES
21(4): S.I (4),863-875, 2026
www.thebioscan.com

investigation therefore aims to: (i) document the taxonomic diversity of cyanobacteria associated with selected rock-cut caves of Nashik District; (ii) compare taxon richness among the cave complexes; (iii) characterize the major morphological groups and their substrate associations; and (iv) discuss the ecological and conservation significance of the observed cyanobacterial assemblages in the context of recent literature.

2. MATERIALS AND METHODS

2.1 Study area

Five cave complexes in Nashik District, Maharashtra, India were included: Chamar Leni Caves, Pandav Leni Caves, Jain Caves in the Anjaneri Hills, Trigalwadi Caves and Ankai Caves. The sites include rock-cut surfaces with variable exposure to water, humidity and illumination. Pandav Leni is situated on Trirashmi Hill near Nashik and comprises 24 rock-cut caves; the official district and state tourism sources identify the complex as an important ancient Buddhist heritage site. The location of the five cave complexes investigated in the present study are shown in figure 1.



Fig. 1: Location map of the five study sites in Nashik District with GPS coordinates and site labels

2.2 Environmental measurements

Temperature was measured using a V&A VA6502 temperature meter. pH was measured using a Hanna Instruments pHep pocket-sized digital pH meter. Relative humidity values reported in the supplied dataset were retained as site-level observations. The recorded environmental conditions were: Chamar Leni, 28 °C, pH 7–8 and 80% humidity; Pandav Leni, 24 °C, pH 7–8 and 97% humidity; Jain Caves, 19 °C, pH 7–8 and 94% humidity; Trigalwadi Caves, 23 °C, pH 9–9.1 and 80% humidity; and Ankai Caves, 27 °C, pH 8.9–9.0 and 77% humidity.

2.3 Sample collection and preservation

Cyanobacterial material was collected from visible growths on cave walls, rock surfaces, wet floors, moist sculptures, soil-associated surfaces, water-contact areas and nearby subaerophytic substrates using non-hazardous collection procedures. Samples were preserved in 4% formalin.

2.4 Microscopic examination and morphometry

Preserved material was examined using a Leica DM3000 trinocular microscope (Germany) equipped with computer imaging. Microphotographs and morphometric measurements were obtained using Leica LAS EZ software. Morphological characters considered included colony organization, mucilage or sheath development, cell shape and dimensions, trichome organization, branching pattern, constriction at cross-walls, apical-cell morphology, heterocyst morphology and occurrence, and general thallus form.

2.5 Taxonomic identification

Taxonomic identification was performed by comparison of observed morphological characters with standard cyanobacterial

taxonomic literature and relevant research papers. The supplied study originally cited Desikachary (1959), Komárek and Anagnostidis (1998, 2005), and Komárek (2013). For the present manuscript, emphasis is placed on post-2000 taxonomic literature and on modern nomenclatural concepts. Cyanobacterial taxonomy has undergone substantial revision through molecular and polyphasic approaches; consequently, historical morphogenera such as *Phormidium*, *Lyngbya*, *Gloeocapsa* and related groups may not correspond directly to monophyletic molecular lineages. The present species list should therefore be interpreted as a morphology-based checklist rather than a definitive molecular taxonomy.

2.6 Data compilation and analysis

The supplied site checklist was transcribed and standardized. Species richness was calculated as the number of distinct morphotaxa recorded at each cave complex. Site occurrence was treated as presence/absence. The compiled checklist contains 55 distinct morphotaxa and 72 site-level occurrence records. The relative contribution of the three morphological groups was calculated from the number of distinct taxa assigned to each group.

3. RESULTS

3.1 Environmental conditions of the study sites

The environmental parameters of temperature, pH, and relative humidity varied significantly between the five explored cave sites resulting in the differences in cyanobacterial microhabitats (Table 1). Specifically, the Chamar Leni Caves showed a temperature of 28°C, a slightly acidic or alkaline pH of 7-8, and 80% relative humidity. The researchers found that cyanobacteria dominated wet rocks with drips, walls, grass, and moss. Meanwhile, the Pandav Leni Caves were characterized by a lower temperature (24°C), a slightly alkaline pH (7-8), and the highest relative humidity (97%). The scientists registered four major microhabitats at this site including moist rocks, walls, sculptural surfaces, and water.

The Jain Caves at Anjaneri Hills were the coolest (19°C) and the most humid (94% relative humidity). The pH level was slightly alkaline (7-8) while the four types of microhabitats included wet rock walls, running water, bark, and caves. The Trigalwadi Caves were slightly alkaline (pH 9.0-9.1), moderately warm (23°C), and moderately humid (80%). The scientists explored wet floors, soil, streams, and walls as the common microhabitats for this site. Finally, the Ankai Caves were the warmest (27°C), slightly alkaline (pH 8.9-9.0), and the least humid (77%). The researchers found moist to wet walls, floors, and the cave's exterior as the common microhabitats for this site.

The examined caves varied significantly in terms of temperature (19-28°C), pH (7.0-9.1), and relative humidity (77-97%). Thus, the environmental conditions were different between the explored caves which likely resulted in the differences in the distribution of the cyanobacterial community.

Table 1: Environmental Conditions of the Studied Cave Sites

Study site	Temperature (°C)	pH	Relative humidity (%)	Representative microhabitats
Chamar Leni Caves	28	7-8	80	Wet dripping rock/walls; wet grass and moss
Pandav Leni Caves	24	7-8	97	Moist rock, cave walls, sculptures, water-contact zones
Jain Caves (Anjaneri Hills)	19	7-8	94	Wet rock walls, flowing-water zone, bark, cave cavities
Trigalwadi Caves	23	9-9.1	80	Wet floor, soil, flowing stream, cave wall
Ankai Caves	27	8.9-9.0	77	Moist/wet walls, floor and outer cave surfaces

3.2 Taxonomic richness

The site-wise distribution of the recorded cyanobacterial taxa was found to be highly variable among the five investigated cave sites (Table 2). Pandav Leni Caves harbored the highest cyanobacterial diversity with 33 taxa, representing 60.0% of the total checklist. The Ankai Caves had 18 cyanobacterial taxa (32.7%), indicating comparatively high diversity in that site. Jain Caves recorded 8 taxa (14.5%), while Chamar Leni Caves and Trigalwadi Caves showed relatively lower numbers with 7 taxa (12.7%) and 6 taxa (10.9%), respectively. Overall, the marked differences in taxon occurrence among the sites may be attributed to varying local environmental conditions and the availability of suitable microhabitats, which may influence the distribution and establishment of cyanobacterial communities within the studied caves.

Table 2: Site-wise Distribution of Cyanobacterial Taxa

Site	Observed taxa	Percentage of total checklist
Chamar Leni	7	12.7
Pandav Leni	33	60.0
Jain Caves	8	14.5
Trigalwadi	6	10.9
Ankai	18	32.7

The observed number of cyanobacterial morphotaxa differed among the five cave complexes, with the highest richness recorded at Pandav Leni (33 morphotaxa), followed by Ankai (18), Jain Caves (8), Chamar Leni (7), and Trigalwadi (6) (Figure 3).

Figure 3. Observed Cyanobacterial Morphotaxon Richness Across Five Cave Complexes

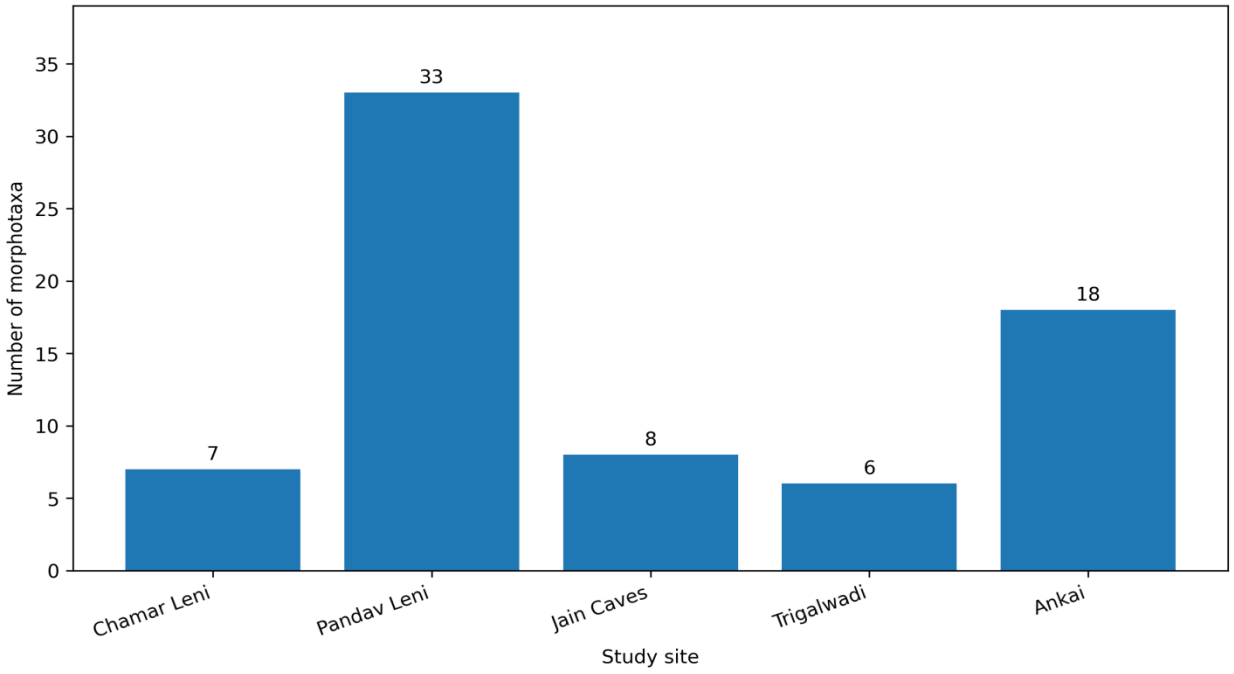


Fig.3: Observed cyanobacterial morphotaxon richness across the five cave complexes

3.3 Composition by morphological group

The recorded cyanobacterial taxa were grouped into three major morphological categories on the basis of their characteristic cellular and filamentous features (Table 3). Coccoid cyanobacteria accounted for the largest group of 25 (45.5%) species of the checklist. Heterocystous cyanobacteria comprised 17 (30.9%) species, while non-heterocystous filamentous cyanobacteria (traditional classification as Oscillatoriales) made up 13 (23.6%) species. Altogether, the checklist comprised 55 species (100%), indicating that coccoid form was the dominant type of cyanobacteria in the studied cave habitats, followed by the heterocystous and non-heterocystous filamentous ones.

Table 3: Morphological Groups of Recorded Cyanobacterial Taxa

Morphological group	No. of taxa	Percentage (%)
Coccoid	25	45.5
Non-heterocystous filamentous (traditionally Oscillatoriales)	13	23.6
Heterocystous	17	30.9
Total	55	100.0

The recorded assemblage comprised 25 coccoid morphotaxa (45.5%), 13 non-heterocystous filamentous morphotaxa (23.6%), and 17 heterocystous morphotaxa (30.9%), giving a total of 55 morphotaxa (Figure 4).

Figure 4. Relative Contribution of Cyanobacterial Morphological Groups

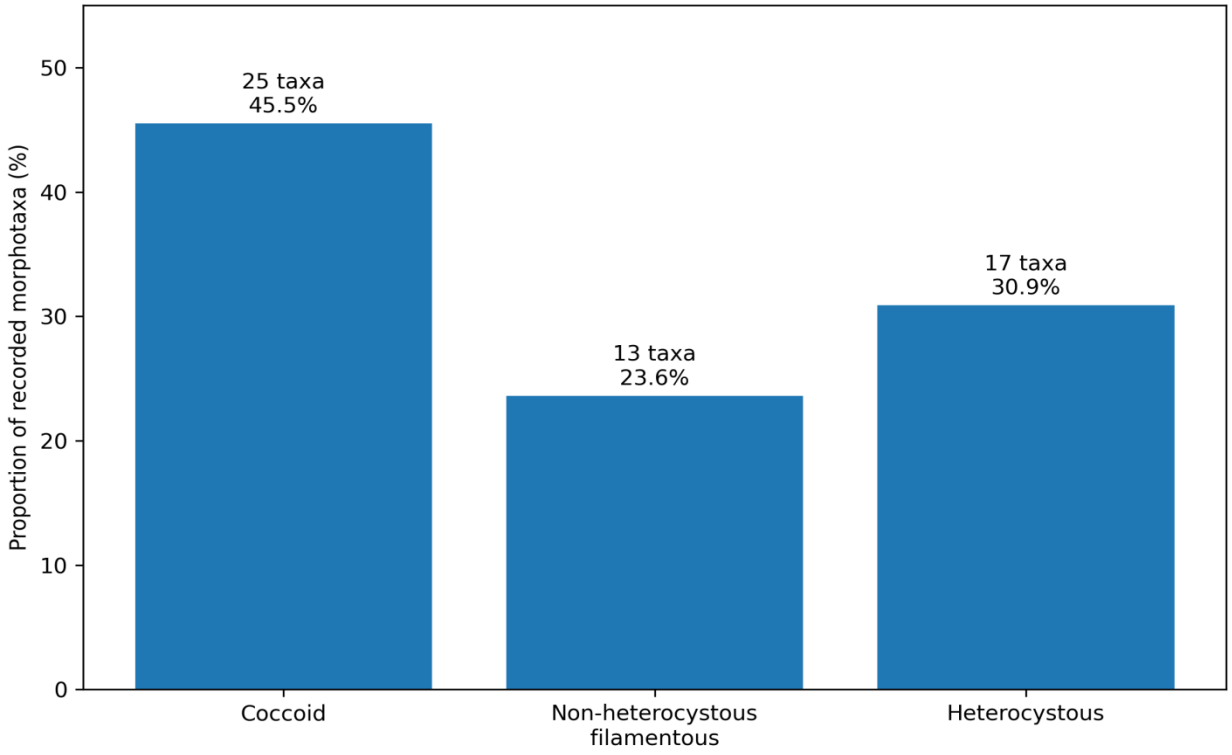


Fig. 4: Relative contribution of coccoid, non-heterocystous filamentous, and heterocystous cyanobacterial morphotaxa

3.4 Distribution across cave complexes

The occurrence of selected cyanobacterial taxa was found to be variable among the five investigated cave sites (Table 4). *Aphanothece castagnei* was recorded from all five sites, suggesting its wide distribution in the study area. *Aphanocapsa parietina* occurred at Chamar Leni, Pandav Leni, and Jain Caves, while *Gloeocapsa compacta* was found in Pandav Leni, Trigalwadi, and Ankai Caves. *Gloeothece confluens* was recorded from Pandav Leni and Ankai Caves.

Table 4: Site-wise Occurrence of Selected Cyanobacterial Taxa

Taxon	Chamar	Pandav	Jain	Trigalwadi	Ankai
Aphanothece castagnei	Chamar	Pandav	Jain	Trigalwadi	Ankai
Aphanocapsa parietina	Chamar	Pandav	Jain	-	-
Gloeocapsa compacta	-	Pandav	-	Trigalwadi	Ankai
Gloeothece confluens	-	Pandav	-	-	Ankai
Phormidium papyraceum	-	Pandav	-	-	Ankai
Phormidium retzii	-	Pandav	Jain	-	-
Oscillatoria princeps	-	Pandav	-	Trigalwadi	-
Scytonema tolypothrichoides	-	Pandav	-	-	Ankai
Nostoc sphaericum	-	Pandav	-	Trigalwadi	-
Nostoc commune	Chamar	Pandav	Jain	Trigalwadi	Ankai

Phormidium papyraceum was detected from both Pandav Leni and Ankai, while *Phormidium retzii* occurred at Pandav Leni and Jain Caves. *Oscillatoria princeps* was found in Pandav Leni and Trigalwadi, whereas *Scytonema tolypothrichoides* was also present in Pandav Leni and Ankai. The heterocystous cyanobacterium *Nostoc sphaericum* occurred at Pandav Leni and Trigalwadi, while *Nostoc commune* was distributed widely in all five sites.

The occurrence data suggest that some taxa were widely distributed in multiple cave habitats while others were restricted to certain sites. Pandav Leni appeared to have the occurrence of most of the taxa reported in Table 4. It is likely due to its diverse and highly humid microhabitats which may be supportive for a comparatively broader range of cyanobacterial forms. The occurrence patterns of the recorded morphotaxa across the five cave complexes are summarized in Figure 5, which highlights taxa shared among sites and those recorded at individual locations.

(ISSN: 0973-7049(P))

The Bioscan
AN INTERNATIONAL QUARTERLY JOURNAL OF LIFE SCIENCES

21(4): S.I (4),863-875, 2026

www.thebioscan.com

Figure 5. Occurrence of Cyanobacterial Morphotaxa Across Five Cave Complexes

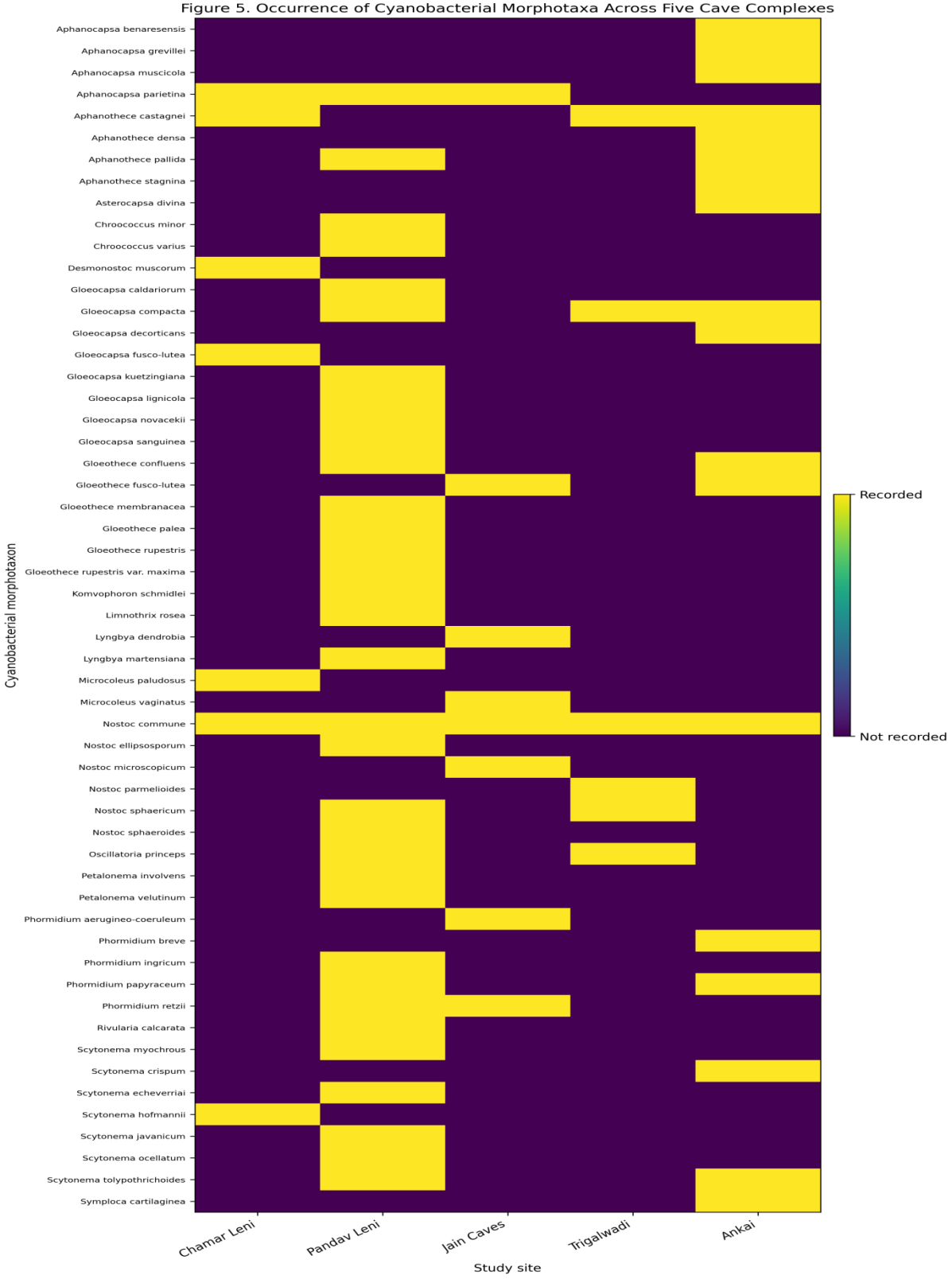


Fig.5: Presence-absence heatmap of 55 cyanobacterial morphotaxa across the five cave complexes. Dark/light cells should be explained in the figure legend

(ISSN: 0973-7049(P))

The Bioscan AN INTERNATIONAL QUARTERLY JOURNAL OF LIFE SCIENCES 21(4): S.I (4),863-875, 2026 www.thebioscan.com

3.5 Taxonomic composition and site-wise distribution

The checklist of taxa comprised 55 cyanobacterial morphotaxa, distributed across the five investigated cave sites (Table 5). The recorded taxa represent a diverse assemblage of coccoid, non-heterocystous filamentous, and heterocystous forms, several of which were restricted to a single cave site, whereas others were distributed across two or more sites.

Table 5: Taxonomic Checklist and Site-wise Distribution of Cyanobacteria

Name of Species and Sites of Collection	C.C	P.C	J.C	T.C	A.C
Aphanocapsa benaresensis Bharadwaja 1935					✓
Aphanocapsa grevillei (Berkeley) Rabenhorst 1865					✓
Aphanocapsa muscicola (Meneghini) Wille 1919					✓
Aphanocapsa parietina Nägeli 1849	✓		✓		
Aphanothece castagnei (Brebisson) Rabenhorst 1865	✓			✓	✓
Aphanothece densa Lemes-da-Silva *et al.*, Acta Bot. Bras. 24(4): 917, 2010					✓
Aphanothece pallida (Kützing) Rabenhorst 1863		✓			✓
Aphanothece stagnina (Sprengel) A. Braun in Rabenhorst 1863					✓
Asterocapsa divina Komárek 1993					✓
Chroococcus minor (Kützing) Nägeli 1849		✓			
Chroococcus varius A. Braun in Rabenhorst 1861		✓			
Desmonostoc muscorum (Agardh ex Bornet *et* Flahault) Hrouzek *et* Ventura 2013	✓				
Gloeocapsa caldariorum Rabenhorst 1865		✓			
Gloeocapsa compacta Kützing 1845		✓		✓	✓
Gloeocapsa decorticans (A. Braun) Richter in Wille 1925					✓
Gloeocapsa fusco-lutea Nägeli 1849	✓				
Gloeocapsa kuetzingiana Nägeli 1849		✓			
Gloeocapsa lignicola Rabenhorst 1865		✓			
Gloeocapsa novacekii Komárek *et* Anagnostidis 1995		✓			
Gloeocapsa sanguinea (Agardh) Kützing 1843		✓			
Gloeothece confluens Nägeli 1849		✓			✓
Gloeothece fusco-lutea Nägeli 1849			✓		✓
Gloeothece membranacea (Rabenhorst) Bornet 1892		✓			
Gloeothece palea (Kützing) Rabenhorst 1865		✓			
Gloeothece rupestris (Lyngbye) Bornet in Wittrock *et* Nordstedt 1880		✓			
Gloeothece rupestris var. maxima after Gonzalves & Kamat (1958)		✓			
Komvophoron schmidlei (Jaag) Anagnostidis *et* Komárek 1988		✓			
Limnothrix rosea (Utermöhl) Meffert 1988		✓			
Lyngbya dendrobia Brühl *et* Biswas 1923			✓		
Lyngbya martensiana Meneghini ex Gomont 1892		✓			
Microcoleus paludosus Gomont ex Gomont 1892	✓				
Microcoleus vaginatus Gomont ex Gomont 1892			✓		
Nostoc commune Vaucher ex Bornet *et* Flahault 1888	✓	✓	✓	✓	✓
Nostoc ellipsosporum (Desmazières) Rabenhorst ex Bornet *et* Flahault 1888		✓			
Nostoc microscopicum Carmichael ex Bornet *et* Flahault 1888			✓		
Nostoc parmelioides Kützing ex Bornet *et* Flahault 1888				✓	
Nostoc sphaericum Vaucher ex Bornet *et* Flahault 1888		✓		✓	
Nostoc sphaeroides Kützing ex Bornet *et* Flahault 1888		✓			
Oscillatoria princeps Vaucher ex Gomont 1892		✓		✓	
Petalonema involvens (A. Braun) Migula 1907		✓			
Petalonema velutinum (Rabenhorst) Migula 1907		✓			
Phormidium aerugineo-coeruleum (Gomont) Anagnostidis *et* Komárek 1988			✓		
Phormidium breve (Kützing ex Gomont) Anagnostidis *et* Komárek 1988					✓
Phormidium ingricum (Voronichin) Anagnostidis *et* Komárek 1988		✓			
Phormidium papyraceum Gomont ex Gomont 1892		✓			✓
Phormidium retzii (Agardh) Gomont ex Gomont 1892		✓	✓		
Rivularia calcarata (Voronichin) Poljanskij in Hollerbach et al. 1953		✓			
Scytonema (Myochrotes) myochrous (Dillwyn) C.A. Agardh ex Bornet *et* Flahault 1886		✓			
Scytonema crispum (Agardh) Bornet 1889					✓
Scytonema echeverriai Kufferath 1929		✓			
Scytonema hofmannii Agardh ex Bornet *et* Flahault 1887	✓				
Scytonema javanicum (Kützing) Bornet *et* Thuret ex Bornet *et* Flahault 1887		✓			
Scytonema ocellatum (Dillwyn) Lyngbye ex Bornet *et* Flahault 1887		✓			
Scytonema tolypothrichoides Kützing sensu Frémy 1927		✓			✓
Symploca cartilaginea Gomont ex Gomont 1892					✓

Among all taxa recorded, *Nostoc commune* was the most widespread species, distributed across all five study sites, whereas *Aphanothece castagnei*, *Aphanothece pallida*, *Gloeocapsa compacta*, *Gloeothece confluens*, *Gloeothece fusco-lutea*, *Nostoc sphaericum*, *Oscillatoria princeps*, *Phormidium papyraceum*, *Phormidium retzii*, and *Scytonema tolypothrichoides* occurred at two or more sites. Overall, the distribution pattern reflects a combination of site-specific and widely distributed cyanobacterial taxa, which indicates differences in habitat conditions and substrate availability among the investigated cave environments.

3.6 Taxonomic and morphological descriptions

Taxonomic and morphological descriptions of cyanobacterial morphotaxa recorded from the five cave complexes of Nashik

District were compiled based on field observations and microscopic examinations carried out during the current study. The identification was performed considering the observed morphological features, namely, cell shape and size, cell arrangement, colonial formation, presence of mucilaginous envelope, filamentous structure, sheath features, mode of branching and the existence or absence of heterocysts. The descriptions were edited according to the scientific nomenclature used in the taxonomic treatments of non-heterocystous and heterocystous cyanobacteria (Komárek & Anagnostidis, 2005; Komárek, 2013). The recent polyphasic taxonomic studies have emphasized the relevance of considering both morphological and molecular data for the resolution of closely related and morphologically similar cyanobacterial taxa (Hrouzek *et al.*, 2013; Kumar *et al.*, 2024). Hence, the morphotaxa presented below were identified based on their morphological descriptions. The recorded occurrences of the taxa from Chamar Leni, Pandav Leni, Jain Caves of Anjaneri Hills, Trigalwadi Caves and Ankai Caves were included in their descriptions. The representative microphotographs of the selected morphotaxa are presented in Figure 2, whereas the detailed checklist and their site-wise distribution are given in Table 5.

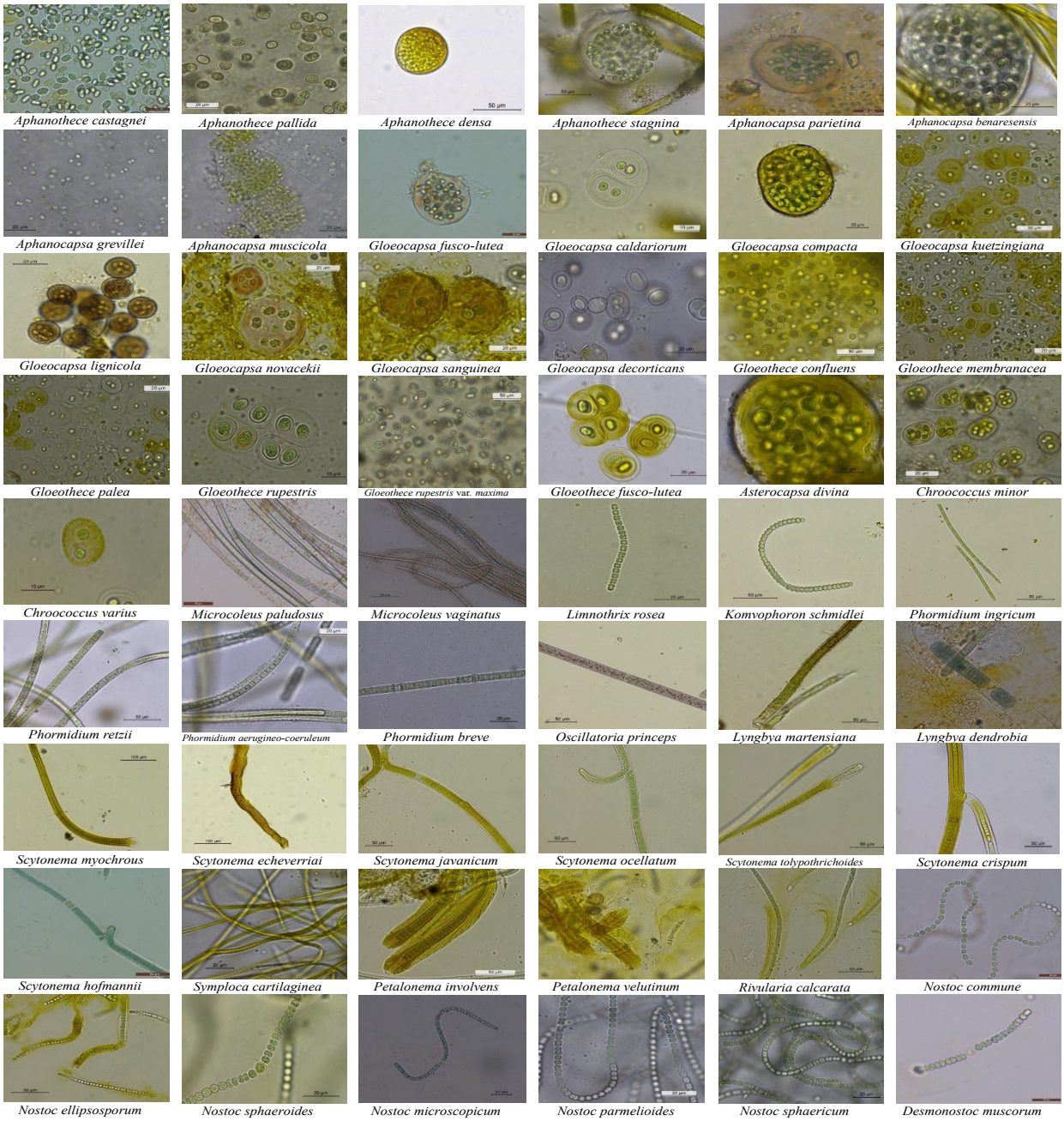


Fig. 2: Representative light microphotograph of selected cyanobacterial morphotaxa recorded from the five cave complexes.

4. CHAMAR LENI CAVES

The cyanobacterial assemblage from Chamar Leni Caves contained seven taxa viz. *Aphanothece castagnei*, *Aphanocapsa parietina*, *Gloeocapsa fusco-lutea*, *Microcoleus paludosus*, *Scytonema hofmannii*, *Nostoc commune* and *Desmonostoc muscorum*. *Aphanothece castagnei* occurred as dark blue-green to olive or yellowish-brown mucilaginous colonies on wet, dripping cave rock. The cells were oval to cylindrical with rounded corners and measured approximately 3.6-4.7 µm in width and 6.9-8.3 µm in length. *Aphanocapsa parietina* formed loosely organized, dirty brownish colonies with pale blue-green cells measuring approximately 4.8-6.2 µm in diameter and was found on or beneath wet cave rock. *Gloeocapsa fusco-lutea* occurred as small irregular yellow-brown subcolonies approximately 40-45 µm in diameter with a slightly lamellate mucilage containing pale blue-green spherical cells of approximately 1.8-2.2 µm diameter. *Microcoleus paludosus* was developed as a dark blue-green thallus on wet substrata, consisting of solitary, unbranched filaments approximately 45-50 µm wide and up to about 1600 µm long. The broad, colourless sheath enclosed parallel rope-like trichomes of approximately 4.9-7 µm in width. *Scytonema hofmannii* formed a cushion-like dark blue-green thallus with filaments approximately 7.5-13.6 µm wide and solitary false branching, the trichomes being cylindrical and approximately 4.8-9.3 µm wide. Solitary or paired heterocysts measured approximately 5.5-9.8 µm in length. *Nostoc commune* formed macroscopic gelatinous colonies, initially spherical but irregular or flattened, with an olive- to brown-green colouration: the cells were barrel-shaped or spherical with terminal and intercalary heterocysts (cells approximately 3.5-4.8 µm wide and 3.8-5.7 µm in length, heterocysts approximately 5.5-7.7 µm wide). *Desmonostoc muscorum* occurred as small hemispherical colonies which developed into mucilaginous olive-green mats containing dense filaments: the colonies possessed a distinct yellowish-brown marginal sheath, with cells measuring approximately 3-5 µm in width and 4-5.4 µm in length and spherical heterocysts approximately 5-6 µm wide. Thus, the Chamar Leni assemblage contained both coccoid and filamentous cyanobacteria, with several taxons found specifically associated with wet and dripping rock surfaces.

5. PANDAV LENI CAVES

Pandav Leni Caves supported the highest taxonomic richness with 33 recorded cyanobacterial taxa. The coccoid and colonial forms contained *Aphanothece pallida*, *Gloeothece confluens*, *Gloeothece membranacea*, *Gloeothece palea*, *Gloeothece rupestris*, *Gloeothece rupestris* var. *maxima*, *Gloeocapsa caldariorum*, *Gloeocapsa compacta*, *Gloeocapsa kuetzingiana*, *Gloeocapsa lignicola*, *Gloeocapsa novacekii*, *Gloeocapsa sanguinea*, *Chroococcus minor* and *Chroococcus varius*: *Aphanothece pallida* formed microscopic greyish to blue-green mucilaginous colonies with loosely arranged oval to cylindrical cells of approximately 5.5-7.2 µm in width and 6.8-10.5 µm in length. *Gloeothece confluens* formed irregular mucilaginous aggregates with colourless non-lamellate envelopes and pale olive-green cylindrical cells of approximately 2.1-3 µm in width and 5.5-7.8 µm in length. *Gloeothece membranacea* consisted of olive-green colonies of clustered cells in common mucilage enclosed by a colourless lamellate envelope (cells approximately 5.1-6.2 µm in width and 8.4-8.8 µm in length). *Gloeothece palea* formed gelatinous colonies containing two to numerous cells of oval to cylindrical cells of approximately 3.2-4 µm in width and 4.2-8.8 µm in length. *Gloeothece rupestris* possessed a distinctly concentrically lamellate common sheath and cells of approximately 3.8-6.7 µm in width and 5-6.6 µm in length, whereas *Gloeothece rupestris* var. maxima formed two-cell colonies with an outer sheath approx. 16.5-20.4 µm diameter and cells of approximately 5-6.5 µm in width and 7.2-10.5 µm in length. *Gloeocapsa caldariorum* formed microscopic aggregated spherical or oval subcolonies containing approx. 4 cells within a thick stratified mucilaginous envelope, the spherical blue-green cells measuring approx. 3.5-7.8 µm in diameter. *Gloeocapsa compacta* formed irregular compact macroscopic colonies with broad mucilage and bright olive-green spherical cells approx. 1.8-3 µm in diameter. *Gloeocapsa kuetzingiana* developed microscopic irregular mucilaginous colonies containing ellipsoidal subcolonies of two to four cells surrounded by a yellow-brown lamellate sheath, cells being approx. 3-4.5 µm in diameter. *Gloeocapsa lignicola* formed crusty globular colonies that were dark mud-brown to blackish, with blue-green spherical cells of approx. 4.5-6.2 µm. *Gloeocapsa novacekii* formed rusty-red mucilaginous colonies approx. 40-60 µm in diameter, with pale olive-green oval or spherical cells approx. 4-8 µm. *Gloeocapsa sanguinea* formed macroscopic gelatinous irregular colonies containing numerous subcolonies, firm lamellate envelopes approx. 120-150 µm in diameter and spherical pale blue-green cells of approx. 3.9-6.2 µm. *Chroococcus minor* formed microscopic irregular colonies of two to four pale blue-green spherical or hemispherical cells of approx. 3-4 µm in diameter whereas *Chroococcus varius* formed microscopic gelatinous colonies of two to four olive-green cells of approx. 2.2-3.8 µm in diameter.

The filamentous non-heterocytous taxa recorded at Pandav Leni were *Limnothrix rosea*, *Komvophoron schmidlei*, *Phormidium ingricum*, *Phormidium papyraceum*, *Phormidium retzii*, *Oscillatoria princeps* and *Lyngbya martensiana*: *Limnothrix rosea* occurred as solitary, slightly curved short trichomes 20-80 µm long, containing 3-20 cells that were barrel-shaped and constricted at cross-walls. *Komvophoron schmidlei* consisted of solitary, slightly curved trichomes approx. 300 µm long and 5-7 µm wide, without a sheath and with conspicuous cross-wall constrictions. *Phormidium ingricum* formed solitary or clustered straight or coiled trichomes measuring approx. 900-1400 µm in length and 3.8-5.3 µm in width, with mostly isodiametric cells and rounded apical cells. *Phormidium papyraceum* developed a thin, dark-green mat with long densely entangled filaments surrounded by a thin papery sheath; the trichomes were generally non-constricted and the cells measured approx. 3.2-5.2 µm in width and 2-4.8 µm in length. *Phormidium retzii* formed a thick compact blackish steel-blue mat with a thin firm colourless sheath, the bright blue-green trichomes being straight or slightly curved and lacking conspicuous cross-wall constrictions. *Oscillatoria princeps* formed a thin blackish to deep blue-green mat with very long, straight or slightly curved motile trichomes, necridia and hormogonia being observed, cells measuring approx. 19-25 µm in width and 3.5-4.7 µm in length. *Lyngbya martensiana* occurred as blue-green entangled filaments arranged parallel to one another, the filaments being approx. 10-11.1 µm wide and enclosed by a thick colourless sheath.

The heterocytous filamentous component at Pandav Leni contained *Scytonema myochrous*, *Scytonema echeverriai*, *Scytonema javanicum*, *Scytonema ocellatum*, *Scytonema tolypothrichoides*, *Petalonema involvens*, *Petalonema velutinum*, *Rivularia calcarata*, *Nostoc commune*, *Nostoc ellipsosporum*, *Nostoc sphaericum* and *Nostoc sphaeroides*: *Scytonema myochrous* formed a flat expanded blackish-green thallus with densely entangled filaments approx. 20-38 µm wide and cylindrical heterocysts approx. 8.5-10 µm wide. *Scytonema echeverriai* formed a thin flat dark blue-green thallus with 30-32 µm wide filaments, a thick yellow-brown sheath, distinctly constricted trichomes and heterocysts approx. 8.6-9 µm in diameter. *Scytonema javanicum* formed a thin cushion-like yellow-brown thallus with erect 11-15.2 µm wide filaments showing geminate or aggregated false branching. *Scytonema ocellatum* produced cushion-like greyish-blue growths with 17.9-18.9 µm wide filaments and geminate or solitary false branching, barrel-shaped heterocysts measuring approx. 9.3-13.6 µm in length and 11-14.2

µm in width. *Scytonema tolypothrichoides* formed dense clusters of coiled or straight repeatedly branched filaments measuring approx. 12-15 µm wide, thick sheaths and elongated barrel-shaped heterocysts. *Petalonema involvens* developed dense fluffy light-brown thalli composed of densely entangled filaments 16.6-25.5 µm wide and possessing broad dirty brownish-yellow lamellated sheaths. *Petalonema velutinum* formed thick dark-brown cushion-like thalli with 12-24 µm wide filaments, fine yellow-brown lamellated sheaths and solitary intercalary spherical heterocysts. *Rivularia calcarata* formed large mucilaginous wart-like olive to yellow-brown colonies, the filaments being approx. 20.4-23 µm wide with regular false branching, funnel-shaped apical sheaths and basal solitary heterocysts measuring approx. 7.9-10.7 µm. *Nostoc ellipsosporum* formed flat granular dark-brown mucilaginous colonies with loosely arranged filaments and yellow-brown sheaths, cells measuring approx. 4.4-5.3 µm in width and 6.4-7.7 µm in length. *Nostoc sphaericum* formed spherical macroscopic colonies approx. 2-3 cm in diameter with a smooth surface and thin periderm, whereas *Nostoc sphaeroides* formed compact gelatinous oval to hemispherical colonies with barrel-shaped cells approx. 4.1-4.9 µm long and 4.7-5.4 µm wide. *Nostoc commune* was also present at this site. Thus, Pandav Leni showed the broadest representation of coccoid, non-heterocytous filamentous and heterocytous cyanobacteria among the investigated cave complexes.

6. JAIN CAVES OF ANJANERI HILLS

The cyanobacterial assemblage of the Jain Caves contained eight taxa viz. *Aphanocapsa parietina*, *Nostoc commune*, *Phormidium retzii*, *Gloeothece fusco-lutea*, *Phormidium aerugineo-coeruleum*, *Microcoleus vaginatus*, *Lyngbya dendrobia* and *Nostoc microscopicum*. *Aphanocapsa parietina* formed loosely organised dirty brownish colonies with pale blue-green cells approx. 4.8-6.2 µm in diameter, occurring on or beneath wet cave rock. *Nostoc commune* formed gelatinous olive- to brown-green colonies with spherical or barrel-shaped cells with terminal or intercalary heterocysts. *Phormidium retzii* was recorded on wet sculpted rock walls and formed a thick compact blackish steel-blue mat with a thin firm colourless sheath, their straight or slightly curved blue-green trichomes lacking conspicuous cross-wall constrictions with cells measuring approx. 5.5-6.4 µm in width and 5-8.8 µm in length. *Gloeothece fusco-lutea* formed small mucilaginous colonies (often with four or eight cells) appearing as brown shiny spots with yellow-brown lamellated envelopes. *Phormidium aerugineo-coeruleum* formed dark blue-green to blackish mucilaginous growths with scattered filaments enclosed by a fine thick colourless sheath, trichomes being approx. 4.5-5 µm wide with cells approx. 3-3.5 µm long. *Microcoleus vaginatus* occurred as solitary creeping curved dark blue-green filaments with attenuated ends and a thick rough colourless sheath bearing hair-like structures, rope-like trichomes being approx. 5.5-6.1 µm wide. *Lyngbya dendrobia* formed a thin papery brownish layer on the substratum, the sheath becoming brownish and thicker with age, dark olive-green trichomes measuring approx. 8.8-10 µm in width with cells approx. 4-6 µm long. *Nostoc microscopicum* formed smooth spherical to ellipsoidal olive-green or brown colonies up to approx. 1 cm in diameter, densely entangled filaments, yellowish to brownish sheaths, cells approx. 3.5-4.4 µm long and 5.2-5.9 µm wide and heterocysts approx. 6.4-8 µm. Thus, the assemblage at Jain Caves was characterised by a mixture of mucilage-forming coccoid taxa and filamentous forms associated with wet rock and sculpted surfaces.

7. TRIGALWADI CAVES

The cyanobacterial flora of Trigalwadi Caves contained six taxa viz. *Gloeocapsa compacta*, *Oscillatoria princeps*, *Nostoc commune*, *Nostoc sphaericum*, *Nostoc parmelioides* and *Gloeothece fusco-lutea*. *Gloeocapsa compacta* formed irregular compact macroscopic colonies with broad mucilaginous envelopes and bright olive-green spherical cells approx. 1.8-3 µm in diameter. The taxon was recorded on wet soil and wall-associated substrates at Trigalwadi. *Oscillatoria princeps* formed a thin blackish to deep blue-green mat composed of very long straight or slightly curved motile trichomes with no conspicuous cross-wall constrictions, necridia and hormogonia being observed; cells approx. 19-25 µm wide and 3.5-4.7 µm long. *Nostoc commune* formed gelatinous olive- to brown-green colonies with spherical or barrel-shaped cells and terminal and intercalary heterocysts and was recorded on wet wall, floor, soil and grass-associated substrates. *Nostoc sphaericum* formed spherical macroscopic colonies approx. 2-3 cm in diameter, smooth surfaced, thin periderm, olive to yellow-brown colouration, densely entangled trichomes and spherical or oval heterocysts. *Nostoc parmelioides* formed spherical or irregular, often flattened brownish colonies with entangled filaments and pale sheaths, cells being barrel-shaped or spherical approx. 3.2-4.1 × 4-4.5 µm with large spherical or slightly elongated heterocysts. *Gloeothece fusco-lutea* was recorded as small mucilaginous colonies containing four or eight cells and surrounded by yellow-brown distinctly lamellated envelopes. Thus, the Trigalwadi assemblage was represented by both coccoid and heterocytous/non-heterocytous filamentous forms with prominent contribution of *Nostoc* taxa.

8. ANKAI CAVES

The cyanobacterial assemblage at Ankai Caves contained 18 taxa viz. *Aphanothece pallida*, *Gloeothece confluens*, *Gloeocapsa compacta*, *Phormidium papyraceum*, *Scytonema tolypothrichoides*, *Gloeothece fusco-lutea*, *Aphanothece densa*, *Aphanothece stagnina*, *Aphanocapsa benaresensis*, *Aphanocapsa grevillei*, *Aphanocapsa muscicola*, *Gloeocapsa decorticans*, *Asterocapsa divina*, *Phormidium breve*, *Symploca cartilaginea*, *Scytonema crispum*, *Nostoc commune* and the additional recorded taxa represented in the site observations. *Aphanothece pallida* formed microscopic greyish to blue-green mucilaginous colonies with loosely arranged oval to cylindrical cells, approx. 5.5-7.2 µm wide and 6.8-10.5 µm long. *Gloeothece confluens* formed irregular mucilaginous aggregates with colourless non-lamellate envelopes and pale olive-green cylindrical cells approx. 2.1-3 µm wide and 5.5-7.8 µm long. *Gloeocapsa compacta* occurred as irregular compact colonies with bright olive-green spherical cells approx. 1.8-3 µm in diameter. *Phormidium papyraceum* formed a thin dark-green mat of long densely entangled filaments enclosed by thin papery sheaths, cells measuring approx. 3.2-5.2 µm in width and 2-4.8 µm in length. *Scytonema tolypothrichoides* formed dense clusters of repeatedly branched filaments measuring approx. 12-15 µm wide, thick sheaths and elongated barrel-shaped heterocysts. *Gloeothece fusco-lutea* formed small mucilaginous colonies with yellow-brown lamellated envelopes and pale blue-green oval to cylindrical cells. *Aphanothece densa* formed microscopic dark brownish mucilaginous colonies with densely arranged cells surrounded by a prominent yellowish-brown sheath, cells measuring approx. 3.5-6.9 µm in length and 3.9-5 µm in width. *Aphanothece stagnina* occurred as dark olive-green mucilaginous spherical or irregular shiny masses with cells more densely arranged at the periphery, approx. 4.5-5.4 µm wide and 7.1-9.3 µm long. *Aphanocapsa benaresensis* formed microscopic hollow, shiny, mucilaginous spherical colonies with greyish blue-green cells approx. 4.2-5.7 µm in diameter. *Aphanocapsa grevillei* formed microscopic gelatinous green colonies with densely arranged spherical to oval bright blue-green cells approx. 3.4-5.2 µm. *Aphanocapsa muscicola* formed irregular mucilaginous colonies ranging from yellowish to dark blue-green or olive-green, compact cells approx. 2-4.1 µm in diameter. *Gloeocapsa decorticans* formed microscopic to macroscopic colourless jelly-like colonies containing one to eight cells per subcolony, surrounded by wide colourless lamellate envelopes, cells spherical or ellipsoidal approx. 6.4-8.2 µm in diameter. *Asterocapsa divina*

occurred as irregular yellowish-brown granular mats approx. 85-115 µm in diameter with a thick golden-brown sheath and spherical to polygonal cells measuring approx. 6.9-7.5 µm wide and 7.1-8.6 µm long without the sheath. *Phormidium breve* formed a dark blue-green mat containing short straight or slightly curved trichomes without cross-wall constrictions, necridia present and cells approx. 1.8-3.4 µm long. *Symploca cartilaginea* formed dense parallel straight filaments producing a bunch-like dark blue-green growth; trichomes approx. 2.6-3.4 µm wide and cells 3.2-4.9 µm long with obtuse-conical apical cells. *Scytonema crispum* formed a cushion-like, woolly, dense green to brownish thallus with filaments approx. 22-32.3 µm wide and predominantly geminate false branching; trichomes distinctly constricted with heterocysts occurring singly or in rows. *Nostoc commune* was also recorded at Ankai on wet wall, floor, soil and grass-associated substrates. Thus, the Ankai assemblage included a substantial representation of mucilage-forming coccoid taxa along with filamentous and heterocytous cyanobacteria, particularly members of *Aphanothece*, *Aphanocapsa*, *Gloeocapsa*, *Phormidium* and *Scytonema*.

Across the five investigated cave complexes, the cyanobacterial assemblages showed considerable variation in taxonomic richness and morphological composition. Pandav Leni exhibited the highest richness with 33 taxa, followed by Ankai with 18 taxa, Jain Caves with 8 taxa, Chamar Leni with 7 taxa and Trigalwadi with 6 taxa. *Nostoc commune* was the only taxon recorded from all five sites, whereas several other taxa were restricted to one or two cave complexes. The site-wise distribution shows that the cyanobacterial communities consisted of a mixture of coccoid mucilage-forming forms, non-heterocytous filamentous forms and heterocytous cyanobacteria, with the relative representation of these groups varying among the cave complexes.

9. DISCUSSION

9.1 Cyanobacterial diversity of the Nashik cave complexes

The checklist of 55 morphotaxa illustrates the substantial morphological diversity among cyanobacteria associated with the selected Nashik caves. The dominance of coccoid taxa in the checklist is notable as compact mucilaginous colonies and thick envelopes can provide protection against desiccation and fluctuating surface conditions. At the same time, heterocystous forms represented almost one-third of the checklist, indicating that nitrogen-fixing cyanobacteria are an important component of the lithic and subaerophytic communities sampled.

The exceptionally high observed richness at Pandav Leni should be interpreted cautiously. The supplied record contains many individual cave numbers, microhabitats and water-associated locations for this site, whereas the sampling intensity at the other sites is not noted with equivalent detail. Therefore, Pandav Leni cannot be described as intrinsically more diverse without standardized sampling effort. This is a methodological issue that should be addressed in a revised field study.

The occurrence of *Nostoc commune* at all five sites suggests broad ecological tolerance within the observed dataset. However, presence at multiple sites does not by itself establish ecological dominance because abundance, biomass and frequency within each microhabitat were not quantified. A future survey should therefore report relative abundance or percent cover in addition to presence/absence.

9.2 Environmental conditions and habitat association

The recorded sites were generally neutral to alkaline. Pandav Leni and Jain Caves showed the highest reported relative humidity (97% and 94%, respectively), whereas Ankai had the lowest humidity (77%). Trigalwadi had the highest pH range (9–9.1), whereas Chamar Leni, Pandav Leni and Jain Caves were approximately neutral to mildly alkaline (pH 7–8). These measurements indicate strong microclimatic heterogeneity among cave systems.

Cyanobacterial persistence on stone is closely related to water availability, irradiance, substrate characteristics and repeated wetting–drying cycles. Modern studies emphasize that phototrophic microorganisms frequently act as pioneer colonizers of stone heritage, while subsequent microbial succession can produce more complex biofilms. Environmental manipulation can also alter microbial outbreaks; for example, high-throughput sequencing at Beishiku Temple showed that changes in shading, temperature and humidity were associated with cyanobacterial proliferation (Zhang *et al.*, 2024). Thus, the high humidity recorded in Pandav Leni and Jain Caves may partly explain the extensive occurrence of moisture-associated morphotypes, although causal relationships cannot be established from the present observational dataset.

9.3 Morphological adaptations relevant to cave surfaces

Several morphological features observed in the dataset are consistent with survival on exposed or periodically desiccated lithic surfaces. These include thick mucilaginous envelopes in *Gloeocapsa* and *Gloeothece*, extensive sheaths in *Microcoleus* and *Lyngbya*, false branching and thick sheaths in *Scytonema*, and gelatinous colonies in Nostoc. Such extracellular matrices can enhance adhesion and water retention. Rossi *et al*. (2012) showed that monument-associated cyanobacteria produce complex extracellular polysaccharides, supporting the ecological importance of the sheath/EPS phenotype in lithophytic biofilms.

The occurrence of *Scytonema* and other heterocystous cyanobacteria is ecologically relevant because heterocyst formation can facilitate nitrogen fixation when combined nitrogen is limited. The lithic environment is often nutrient-poor, and nitrogen-fixing phototrophs may therefore contribute to early nutrient accumulation within developing biofilms. Nevertheless, nitrogen fixation was not experimentally measured in the present study and should not be inferred for every heterocystous taxon solely from morphology.

9.4 Comparison with Indian monument studies

The present assemblage overlaps conceptually with earlier Indian studies of cyanobacteria on cultural stone. Keshari and Adhikary (2014) reported 24 species belonging to 11 genera from Indian temples, caves, mortar monuments and building facades, with genera such as *Scytonema*, *Lyngbya* and related filamentous forms contributing prominently to biofilms. Rossi *et al*. (2012) showed that cyanobacteria isolated from the Parasurameswar Temple and Khandagiri Caves produced extracellular polysaccharides with multiple neutral and acidic sugars. These findings support the interpretation that the sheathed and mucilaginous taxa observed in Nashik may contribute to persistent surface biofilms.

The Nashik checklist is also broadly consistent with the wider literature showing that cyanobacterial communities on monuments are highly site-specific. Mediterranean monument surveys have reported substantial cyanobacterial and green-algal diversity associated with variations in lithology, microclimate and surface conditions (Macedo *et al.*, 2009). More recent work has moved from morphology solely toward molecular community profiling, revealing that visually similar biofilms can contain phylogenetically distinct organisms. This transition is particularly relevant to the present dataset.

9.5 Taxonomic limitations and need for molecular confirmation

The most important limitation of the present study is that identification was based on morphology. Cyanobacterial taxonomy has undergone extensive revision due to many traditional morphogenera being defined primarily by characters that can vary with culture conditions, environmental stress and developmental

stage. Modern taxonomy increasingly combines morphology with 16S rRNA gene phylogeny, 16S-23S ITS analysis and additional phenotypic characters. Recent Indian work on *Nostoc* and *Desmonostoc* has demonstrated that morphologically similar strains can resolve into different phylogenetic lineages when a polyphasic approach is used (Kumar *et al.*, 2024).

The taxonomic status of *Desmonostoc muscorum* illustrates the importance of nomenclatural updating. The genus *Desmonostoc* was established as a phylogenetically coherent lineage separate from Nostoc based on molecular and morphological evidence (Hrouzek *et al.*, 2013). Similarly, the phylum name Cyanobacteriota has been formally validated under modern nomenclatural treatment (Oren *et al.*, 2022). Accordingly, the present checklist should be described as a morphology-based inventory and should not be interpreted as a definitive species-level molecular inventory.

9.6 Potential significance for conservation of Nashik cave heritage

Cyanobacterial colonization has potential conservation implications due to phototrophic biofilms causing visible discoloration and creating microenvironments favorable to other microorganisms. Reviews of cultural-heritage biodeterioration emphasize that microbial communities may participate in both chemical alteration and physical penetration of stone. Recent research at the Taj Mahal has provided microscopic and spectroscopic evidence of complex cyanobacterial biofilms associated with mineral interactions, while a 2025 metagenomic study emphasized that conservation diagnosis should identify the organisms and metabolic processes that are actually active at a particular monument (Banerjee & Singh, 2026; Ma *et al.*, 2025).

The present study does not directly demonstrate stone deterioration since mineralogical, surface-chemistry, SEM, FTIR, mechanical-strength or controlled biodeterioration measurements were not included. Therefore, terms such as 'biodeteriorative' should be used cautiously. The safer interpretation is that the recorded cyanobacteria represent potential contributors to lithic biofilms and that their conservation significance warrants targeted physicochemical assessment.

9.7 Recommended next phase of the study

For a stronger Web of Science/Scopus-level manuscript, the next phase should have: (1) GPS coordinates and standardized sampling effort; (2) seasonal sampling, preferably pre-monsoon, monsoon/post-monsoon and winter; (3) quantitative abundance or percentage cover; (4) stone type/mineralogy; (5) surface moisture, light intensity and temperature logging; (6) SEM/EDS or confocal microscopy for biofilm–stone interactions; (7) 16S rRNA and 16S-23S ITS sequencing; (8) phylogenetic analyses with reference strains; (9) multivariate statistics linking community composition and environmental variables. These additions would substantially improve taxonomic confidence and ecological interpretation.

10. CONCLUSIONS

The current investigation documents a diverse cyanobacterial assemblage associated with five rock-cut cave complexes of Nashik District, Maharashtra. Fifty-five morphotaxa representing 18 genera and 72 site occurrences were compiled from the provided observations. Pandav Leni demonstrated the highest observed richness, whereas *Nostoc commune* was the only taxon recorded across all five cave complexes. The assemblage included coccoid, non-heterocystous filamentous and heterocystous morphotypes, many of which possessed mucilage, sheaths, false branching or heterocysts that are ecologically compatible with fluctuating lithic microhabitats. The study expands the baseline knowledge of cyanobacterial diversity associated with Nashik's rock-cut heritage. At the same time, the findings should be regarded as a morphology-based inventory. Modern cyanobacterial taxonomy and recent heritage-microbiology studies demonstrate the value of molecular and polyphasic approaches. Molecular confirmation, standardized seasonal sampling and quantitative assessment of stone–biofilm interactions are therefore essential before individual taxa are used as definitive indicators of biodeterioration or conservation risk.

11. REFERENCES

- Banerjee, D., & Singh, M. R. (2026). Biofilm-induced deterioration of marble at the Taj Mahal: Spectroscopic and microscopic evidence of cyanobacterial colonisation. *Built Heritage*, 10, Article 43. https://doi.org/10.1186/s43238-026-00288-2
- Gaylarde, C. C. (2020). Influence of environment on microbial colonization of historic stone buildings with emphasis on cyanobacteria. *Heritage*, 3(4), 1469–1482. https://doi.org/10.3390/heritage3040081
- Hrouzek, P., Lukešová, A., Mareš, J., & Ventura, S. (2013). Description of the cyanobacterial genus *Desmonostoc* gen. nov. including *D. muscorum* comb. nov. as a distinct, phylogenetically coherent taxon related to the genus *Nostoc*. *Fottea*, 13(2), 201–213. https://doi.org/10.5507/fot.2013.016
- Keshari, N., & Adhikary, S. P. (2013). Characterization of cyanobacteria isolated from biofilms on stone monuments at Santiniketan, India. *Biofouling*, 29(5), 525–536. https://doi.org/10.1080/08927014.2013.794224
- Keshari, N., & Adhikary, S. P. (2014). Diversity of cyanobacteria on stone monuments and building facades of India and their phylogenetic analysis. *International Biodeterioration & Biodegradation*, 90, 45–51. https://doi.org/10.1016/j.ibiod.2014.01.014
- Keshari, N., Das, S. K., & Adhikary, S. P. (2021). Colonization and survival of a stress tolerant cyanobacterium on a heritage monument of Santiniketan, India. *International Biodeterioration & Biodegradation*, 164, 105294. https://doi.org/10.1016/j.ibiod.2021.105294
- Komárek, J. (2005). Cyanoprokaryota 2. Teil/2nd Part: Oscillatoriales. In B. Büdel, L. Krienitz, G. Gärtner, & M. Schagerl (Eds.), Süßwasserflora von Mitteleuropa 19/2. *Elsevier/Spektrum*.
- Komárek, J. (2013). Süßwasserflora von Mitteleuropa, Bd. 19/3: Cyanoprokaryota: 3. Teil/3rd part: Heterocytous genera. *Springer Spektrum*.
- Komárek, J., & Anagnostidis, K. (2005). Cyanoprokaryota 2. Teil/2nd Part: Oscillatoriales. In B. Büdel, L. Krienitz, G. Gärtner, & M. Schagerl (Eds.), Süßwasserflora von Mitteleuropa 19/2. *Elsevier/Spektrum*.
- Kumar, N., Saraf, A., Pal, S., & Singh, P. (2024). Expanding the cyanobacterial flora of India: Multiple novel species of *Nostoc* and *Desmonostoc* from Jammu and Kashmir, India using a polyphasic approach. *Journal of Phycology*, 60, 1190–1209. https://doi.org/10.1111/jpy.13498
- Macedo, M. F., Miller, A. Z., Dionísio, A., & Saiz-Jimenez, C. (2009). Biodiversity of cyanobacteria and green algae on monuments in the Mediterranean Basin: An overview. *Microbiology*, 155, 3476–3490.
- Ma, C., Zhang, X., Wu, F., & Liu, X. (2025). Identifying keystone taxa and metabolisms of epilithic biofilms is crucial to the conservation of stone heritage from biodeterioration. *Frontiers in Microbiology*, 16, 1600865. https://doi.org/10.3389/fmicb.2025.1600865
- Mkhinini, M., Versace, D.-L., Abbad-Andalousi, S., Verney-Carron, A., Bousta, F., Bousserrhine, N., Reboah, P., &

Balland, C. (2026). Advanced insights into the biodeterioration and conservation strategies of cultural heritage: A review. *Science of the Total Environment*, 1010, 181029. https://doi.org/10.1016/j.scitotenv.2025.181029

- Negi, A., & Sarethy, I. P. (2019). Microbial biodeterioration of cultural heritage: Events, colonization, and analyses. *Microbial Ecology*, 78, 1014–1029. https://doi.org/10.1007/s00248-019-01366-y
- Oren, A., Mareš, J., & Rippka, R. (2022). Validation of the names Cyanobacterium and Cyanobacterium stanieri, and proposal of Cyanobacteriota phyl. nov. *International Journal of Systematic and Evolutionary Microbiology*, 72(10), 005528. https://doi.org/10.1099/ijsem.0.005528
- Pointing, S. B., & Belnap, J. (2012). Microbial colonization and controls in dryland systems. *Nature Reviews Microbiology*, 10, 551–562.
- Rossi, F., Micheletti, E., Bruno, L., Adhikary, S. P., Albertano, P., & De Philippis, R. (2012). Characteristics and role of the exocellular polysaccharides produced by five cyanobacteria isolated from phototrophic biofilms growing on stone monuments. *Biofouling*, 28(2), 215–224. https://doi.org/10.1080/08927014.2012.663751
- Scheerer, S., Ortega-Morales, O., & Gaylarde, C. (2009). Microbial deterioration of stone monuments—An updated overview. *Advances in Applied Microbiology*, 66, 97–139. https://doi.org/10.1016/S0065-2164(08)00805-8
- Zhang, Y., Wu, F., Gu, J.-D., He, K., Fang, Z., Liu, X., He, D., Ding, X., Li, J., Han, Z., Zhang, Q., & Feng, H. (2024). Dominance by cyanobacteria in the newly formed biofilms on stone monuments under a protective shade at the Beishiku Temple in China. *Environmental Research*, 251, 118576. https://doi.org/10.1016/j.envres.2024.118576